CHEMICAL ENGINEERING RESEARCH AND DESIGN 90 (2012) 86–97

Contents lists available at ScienceDirect

Chemical Engineering Research and Design

journal homepage: www.elsevier.com/locate/cherd

Selectivity engineering in the synthesis of value added chemicals: Oxidation of 1-octanol to 1-octanal over nano-fibrous Ag–OMS-2 catalysts

Ganapati D. Yadav, Rajubhai K. Mewada*

Department of Chemical Engineering, Institute of Chemical Technology Matunga Mumbai 400019 India[1]

ABSTRACT

Oxidation of 1-octanol to 1-octanal is commercially very attractive, since the product is used extensively in the fragrance industry. Among the various methods, selective air oxidation with a suitable heterogeneous catalyst will be green and clean. In this work, novel cryptomelane type octahedral molecular sieve type 2 (Ag–OMS-2) catalysts, with Ag loading from 5 to 15%, w/w, were synthesized and evaluated in air oxidation of 1-octanol in a fixed bed vapour phase reactor. All catalysts were fully characterized to understand the activity and selectivity. The conversion increased with Ag loading but the selectivity was the highest for 10% Ag–OMS-2. A systematic study was conducted to ascertain the effects of various parameters. Use of toluene as a diluant leads to better conversion and selectivity. The optimized conditions are: catalyst mass/molar flow rate of 1-octanol (W/F_{A0})- 20 g h/mol, 523 K, toluene to 1-octanol molar ratio- 4:1, weight hourly space velocity (WHSV)- 16.74 h^{-1}, air flow rate- 6 L/h, air pressure- 101.3 kPa. It follows the Mars-van Krevelen mechanism and is intrinsically kinetically controlled. The activation energy is 14.39 kcal/mol using 10%, w/w Ag–OMS-2. It provides a better green process than those reported so far.

© 2011 The Institution of Chemical Engineers. Published by Elsevier B.V. All rights reserved.

Keywords: Nanocatalysis; Nano-fibrous material; Silver; Octahedral molecular sieve-2(OMS-2); Ag–OMS-2; 1-octanol; Oxidation; 1-Octanal; Mars-van Krevelen mechanism; Selectivity

1. Introduction

Carbonyl compounds have widespread applications in a variety of industries. Oxidation of alcohols is one of the routes which are rampantly used to produce carbonyl compounds. However, selectivity to the desired carbonyl compound is a highly challenging task because it invariably leads to over-oxidation. The selective catalytic oxidation of alcohols using O_2 or H_2O_2 has been proposed as a green methodology to replace the highly polluting processes which employ stoichiometric quantities of inorganic oxidants such as $K_2Cr_2O_7$ and $KMnO_4$ (Sheldon and Kochi, 1981; Mallat and Baiker, 2004).

1-Octanal is used extensively in the fragrance industry and prepared by a variety of synthetic methods. Many patents have appeared on its preparation (Miura et al., 2003; Tanielyan et al., 2004, 2006). Homogeneous catalysts have been used for making 1-octanal and most of the recent literature involves the use of TEMPO ((or 2,2,6,6-tetramethylpiperidin-1-yl)oxyl) based catalysts in liquid phase reactions (Ciriminna and Pagliaro, 2010). Homogeneous catalysts give better conversion and selectivity compared to the heterogeneous catalysts but they suffer from the problem of separation from the reaction mixture and stability under reaction conditions. (Buffin et al., 2005; Che et al., 2006; Coleman et al., 1999; Einhorn et al., 1996; Fritz-Langhals, 2005; Gamez et al., 2003; Gilhespy et al., 2005). Different heterogeneous catalysts have also been used for the synthesis of 1-octanal (Anderson et al., 2003; Bogda and Lukasiewicz, 2000; Ji et al., 2002; Kockritz et al., 2006; Krohn et al., 1996; Noyori et al., 2003; Yamaguchi and Mizuno, 2002). Several reviews have compared various catalysts and their performance in 1-octanal synthesis (Mallat and Baiker, 2004; Muzart, 2003; Zhan and Thompson, 2004). Supported

---

* Corresponding author. Tel.: +91 22 3361 1001/1111/2222; fax: +91 22 3361 1002/1020.
E-mail addresses: gdyadav@yahoo.com, gd.yadav@ictmumbai.edu.in (G.D. Yadav).

Received 18 March 2011; Received in revised form 17 July 2011; Accepted 3 August 2011

[1] Formerly University of Mumbai Institute of Chemical Technology; now a separate University.

0263-8762/$ – see front matter © 2011 The Institution of Chemical Engineers. Published by Elsevier B.V. All rights reserved.
doi:10.1016/j.cherd.2011.08.007

Nomenclature

A	1-Octanol
B	1-Octanal
C	$k_2P_{O_2}$ = constant
C′	Constant
F_{A_0}	molar flow rate of reactant,1-octanol, mol h^{-1}
k_1	Apparent rate constant, mol $gcat^{-1}\,h^{-1}\,m^2\,N^{-1}$
k_2	rate constant for re-oxidation reaction of the catalyst, mol $gcat^{-1}\,h^{-1}\,m^2\,N^{-1}$
L	Air flow, L
N_{A_0}	Initial moles of A
$N_{A,t}$	moles of A time t
$N_{B,t}$	moles of B at time t
P_{A_0}	partial pressure of 1-octanol at starting of the reaction, N/m2 (also Pa),
P_{O_2}	partial pressure of oxygen, N/m^2 (also Pa),
$-r_A$	rate of reaction of 1-octanol, mol $gcat^{-1}\,h^{-1}$
$-r_{O_2}$	rate of reoxidation of the catalyst, mol $gcat^{-1}\,h^{-1}$
S_B	selectivity of 1-octanal
t	time, h
W	weight of the catalyst, g
WHSV	Weight hourly space velocity, h^{-1}
x_A	conversion of 1-octanol at given W/F_{A0} value

Greek letters

θ	degree of catalyst surface occupied by the oxygen (–)

Au, Pd, Pt, and Ru nanoparticles are the major heterogeneous catalysts for the oxidative dehydrogenation of alcohols (Matsumoto et al., 2008; Shi et al., 2010). These catalysts are active for allylic and benzylic alcohols but less active for non-activated substrates like primary aliphatic alcohols. Their large scale application still suffers from the low selectivity due to over-oxidation including the hazards of using flammable solvents. Transfer dehydrogenation of alcohols was recently proposed as a green route with Cu/MgO as catalyst for the conversion of primary aliphatic alcohols (Shi et al., 2010).

Stability of the catalyst under reaction conditions and selectivity to the desired product are major problems associated with heterogeneous catalysts. In liquid phase oxidation reactions, some catalysts give higher conversion and selectivity at low concentration of the substrate; however, they fail to give good conversion at high concentration. Very few reports are available on 1-octanol oxidation in vapour phase (Yang et al., 2005). Due to use of high temperature in vapour phase reactions, over-oxidation normally occurs. Commercially 1-octanal has been produced either by hydroformylation of olefins or direct dehydrogenation process. Vapour phase dehydrogenation process is described using copper–chomite catalyst in the presence of nitrogen. It gives good conversion but poor selectivity (Franz and Sheldon, 2003). A patent by Stamicarbon describes a very stable copper containing catalyst (CuO–MgO) which shows very good activity and selectivity. However, it is a complicated process involving activation of the catalyst (Graaf and Franciscus, 1981).

The foregoing shows that there is a tremendous scope to develop new catalysts and processes to synthesize 1-octanal. Among various octahedral molecular sieves (OMS), cryptomelane OMS-2 has shown good catalytic activity for various oxidation reactions. This catalyst could be modified to improve its activity and stability. This work discusses the vapour phase air oxidation of 1-octanol using a novel catalyst based on octahedral molecular sieves in which different amounts of silver are doped. Synergism of silver with potassium and manganese inside the framework of the OMS-2 improves the activity and selectivity of the catalyst significantly. A kinetic model is also proposed and validated against experimental data. The results are novel and provide an insight into the overall process.

2. Experimental

2.1. *Chemicals*

All chemicals were procured from firms of repute and used without further purification:

1-Octanol, toluene, methanol (AR grade; M/s. S. D. Fine Chem. Ltd., India), air as an oxygen source (GC grade purity, Inox India Ltd.)

2.2. *Catalyst preparation*

The reference catalyst octahedral molecular sieve-2 (K–OMS-2) and the silver substituted OMS-2 (Ag–OMS-2) with varying amounts of Ag were synthesized by precipitation method under acidic conditions.

A 0.5–1.05 mol/L silver nitrate solution (1.5–4.35 g $AgNO_3$ dissolved in 25 mL distilled water) was added to the acidic solution of 1.27 mol/L manganese acetate (21.0 g $Mn(COOCH_3)_2{\cdot}4H_2O$ dissolved in 67.5 mL distilled water) having pH 1. 8–10 mL concentrated nitric acid was used in manganese acetate solution. The amount of silver was selected as per the loading of silver required in the final catalyst, i.e., 5, 10 or 15, w/w% Ag. A 0.37 mol/L potassium permanganate solution (13.3 g $KMnO_4$ dissolved in 225 mL distilled water) was added dropwise in the manganese acetate solution at 343 K. Rigorous stirring was maintained during the addition of $KMnO_4$. The resulting mixture was stirred and refluxed at 373 K for 24 h. The precipitate was washed several times with distilled water to make it neutral. The final solid product was filtered and dried at 393 K for 10 h and calcined at 673 K. The catalysts K–OMS-2 (Zhou et al., 1998) and UDCaT-3 were synthesized by methods reported earlier (Yadav and Maniar, 2008). UDCaT is an acronym of University Department of Chemical Technology, the authors institute's former name which was changed recently. It is a vanadium based OMS-2 prepared in our laboratory.

2.3. *Catalyst characterization*

Thermogravimetry (TGA) and differential thermal analysis (DTA) of the catalysts was carried out with DTG-60 H (Shimadzu, Japan) in aluminum pan. The loss in weight of the catalyst sample was measured during heating from room temperature to 773 K with a ramp rate of 5 K/min under nitrogen flow of 15 mL/min.

Acidic and basic catalytic sites were determined by temperature programmed desorption (TPD) analysis using Autochem II 2910 (Micromeritics, USA) with ammonia and carbon dioxide as probe molecules, respectively. A quantity of 30 mg of the catalyst was taken in a quartz tube and degassed up to 625 K under the flow of nitrogen. Then ammonia or carbon dioxide (as per the required test) was passed for 30 min to adsorb the ammonia or carbon dioxide over the surface of the catalysts at room temperature. Physisorbed gas was removed by passing inert nitrogen at room temperature. Chemisorbed ammonia or carbon dioxide was desorbed by using temperature programmed desorption and detected by TCD.

The reduction nature of the catalyst sample was characterized by temperature programmed reduction analysis (TPR) using Autochem II 2920. The sample was first oxidized to 673 K under a continuous flow of a mixture of 5% oxygen and 95% helium. Then the samples was flushed with nitrogen to remove all physisorbed and excess oxygen from the sample followed by temperature programmed desorption (TPD) up to 673 K.

The surface properties of K–OMS-2 and Ag–OMS-2 were measured by the Brunauer–Emmett–Teller (BET) method using ASAP 2010 (Micromeritics, USA) instrument. Degassing of the samples was carried out under vacuum at 573 K for 4 h. Using liquid nitrogen as the adsorbent, all measurements were made with a multipoint method and isotherms were prepared. Surface area and pore volume were calculated from N_2-adsorption–desorption isotherms using conventional BET and Barrett–Joyner–Halenda (BJH) methods.

Surface morphology of the catalyst samples was captured with scanning electron microscope (SEM) (Camera SU 30 microscope, JEOL, Japan). The dried samples were mounted on specimen studs and sputter coated with a thin film of gold to prevent charring. The gold coated surface was then scanned at various magnifications. The surface composition was measured with an average of three data points at different locations of the solid by energy dispersive X-ray spectroscopy (EDXS) (KEVEX X-ray spectrometer JED-2300, JEOL, Japan).

The crystalline nature of the catalyst was analyzed with X-ray diffraction (XRD) technique with Phillips X'pert System instrument with Cu Kα radiation with a beam current of 40 kV and 100 mA. The XRD patterns were collected from 2θ from 0 to 70.

2.4. *Reaction procedure*

Vapour phase oxidation of 1-octanol was carried out in a fixed bed catalytic reactor made of stainless steel (17.2 mm diameter × 250 mm height) (Chemito Technologies, Mumbai) (Fig. 1). The bed was packed with a known quantity of dry catalyst. Inert glass beads were packed above the catalyst bed. The reactor was equipped with liquid feed pump (HPLC grade, Knauer, USA), a preheater, gas flow arrangement with mass flow controllers and a condenser after the reactor. The temperature of the bed was maintained within ±1 K accuracy. The flow rate of the gas was measured and controlled by mass flow controllers. Samples were collected from the condenser for analysis.

Before each experiment, the catalyst was activated under the flow of air for 2 h at the desired reaction temperature, i.e., 523 to 623 K. The gas and liquid phase mixture (1-octanol and toluene as solvent) was passed through the preheater to achieve the bed temperature and then passed downwards through the catalyst bed. The outgoing vapours were cooled to collect the liquid samples. Typical reaction conditions were: catalyst- 0.5 g, temperature- 598 K, toluene to 1-octanol molar ratio- 4:1, air flow rate- 6 L/h at 303 K and 101 kPa and WHSV of the feed at 303 K, 16.74 h^{-1}.

2.5. *Method of analysis*

Analysis of the reaction mixture was performed by GC (Chemito 8610 model). A 4 m × 3.18 mm internal diameter stainless steel column packed with 10% SE-30 on chomosorb WHP was used for analysis in conjunction with a flame ionization detector. The quantification of the collected data was done though a calibration procedure by using synthetic mixtures and it was used to get conversions, rates of reaction and selectivity. Products were confirmed with GC-MS and authentic samples.

Typical product distribution for 1-octanol oxidation reaction based on GC analysis is given below; conversion and selectivity to 1-octanal were 65 and 98.3%, respectively. The conversions were calculated based on the mol basis using the data obtained from GC analysis.

$$x_A = \frac{N_{A_0} - N_{A,t}}{N_{A_0}} \tag{1}$$

where, x_A, N_{A_0}, and $N_{A,t}$ are fractional conversion, initial moles and moles at any time *t* of octanol, respectively.

Selectivity is defined based on the number of moles of 1-octanal (B, desired product) produced to total number of moles of 1-octanol converted during reaction,

$$S_B = \frac{N_{B,t}}{N_{A_0} - N_{A,t}} \tag{2}$$

where, S_B and $N_{B,t}$ are fractional selectivity to 1-octanal (B, the desired product) and moles of B produced at time *t*. The weight hourly space velocity (WHSV) in h^{-1} is defined as follows:

$$\text{WHSV} = \frac{F}{W} \tag{3}$$

The parameter W/F_{A_0} in g h/mol is also used for evaluating the performance of the catalyst.

Where, F, F_{A0} and W are total mass flow of liquid feed (mixture of toluene and 1-octanol) (g h^{-1}), molar flow of 1-octanol (mol h^{-1}) and mass of catalyst (*g*).

3. Results and discussion

3.1. *Catalyst characterization*

Synthesis of Ag–OMS-2 results in the brownish black fibrous crystalline material at different loadings of Ag into the reference K–OMS-2 material. The synthetic Ag–OMS-2 catalysts have a one-dimensional tunnel structure formed by 2 × 2 edge shared MnO_6 octahedral chains. Thermal stability of all samples was determined with TGA. The weight loss was gradual and catalyst found stable up to 773 K. For sake of brevity these data are not included.

1-Octanol oxidation shows positive effect of silver addition in K–OMS-2. To find the effect of addition of silver in K–OMS-2, acidity, basicity and TPR-TPO studies were carried out. Introduction of silver ions modifies the surface properties of the OMS-2 particles, resulting from the reduction of the number of free hydroxyl groups and deposition of strongly dispersed silver particles on the outer surface of the oxides. Incorporation of small amounts of silver by the direct addition to the synthesis mixture results in partial replacement of potassium ions from the channels which will alter the catalytic properties. Since silver ions are smaller than potassium one, there

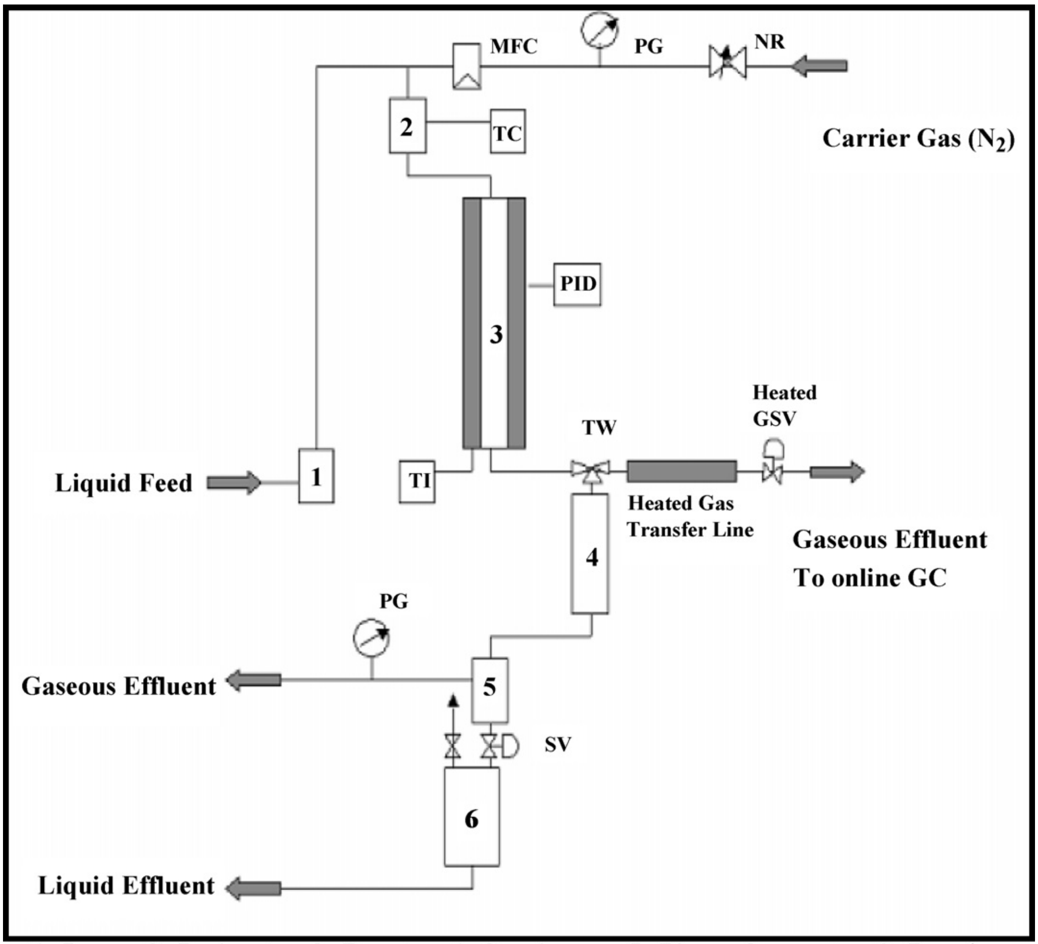

1: Pump, 2: Preheater, 3: Reactor, 4: Condenser, 5: Phase Separator, 6: Receiver

Fig. 1 – Schematic diagram of the experimental setup.

is a likelihood of structural alteration in manganese oxide during their synthesis and thermal treatment, leading to the formation of different sized channels, dislocations or oxygen vacancies. This methodology increases of the surface area and formation of mesoporous structure which have been observed in this study. The presence of silver ions or small silver crystallites can increase the number of active sites on the surface of manganese oxides and improve catalytic properties due to silver–manganese interactions. This has been also observed by Gac (2007) and Gac et al. (2008).

TPD analysis, with ammonia and carbon dioxide as probe molecules, confirmed the existence of mild acidic and basic sites of Ag–OMS-2. In OMS-2 based catalysts, the existence of manganese in a mixture of oxidation states (+2, +3, and +4) is known. Addition of Ag inside the catalyst structure replaces K and decreases the strong acidic sites and makes it mildly acidic. It is observed that increasing the loading of silver ion from 5 to 15%, w/w increases number of weak active sites. Two different peaks at lower temperature (Figs. 2 and 3) confirm the existence of two different types of acidic sites, one each for Mn^{4+} and Ag^{+}. However, only one peak appeared in CO_2 TPD profile. Also the basic sites are provided by Mn^{4+}. In Ag–OMS-2 catalyst, manganese exists in mixed valency, Mn^{3+} (Mn_2O_3) and Mn^{4+} (MnO_2). In our case, Ag^{+} ions have been incorporated in the tunnel structure of OMS-2. The peaks below 100 °C are due to physisorbed NH_3/CO_2.

During TPD, TPR or TPO study, due care was taken to avoid any physical adsorption. All TPD curves show low temperature peak at 110–120 °C. That is due to weak acid sites present on the catalyst surface. On addition of silver from 0% to 10% on K–OMS-2, the amount of NH_3 or CO_2 adsorbed increased. Change in redox nature of K–OMS-2 after addition of silver is observed as shown in Fig. 4. Addition of 5% silver in K–OMS-2 catalyst results in decrease in reduction temperature of K–OMS-2 significantly from 553 to 423 K (Fig. 4). The same trend was also observed for 10% Ag–OMS-2 and 15% Ag–OMS-2 also. This is in consonance with those observed by others (Fu

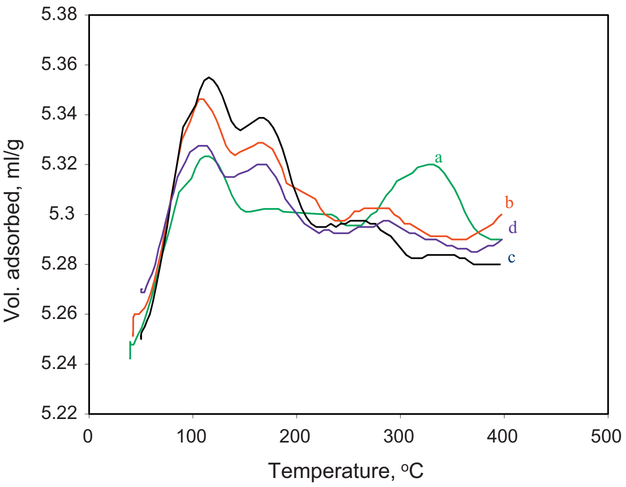

Fig. 2 – Ammonia TPD profiles for various catalysts (a) K–OMS-2, (b) 5%Ag–OMS-2, (c) 10% Ag–OMS-2, (d) 15%Ag–OMS-2.

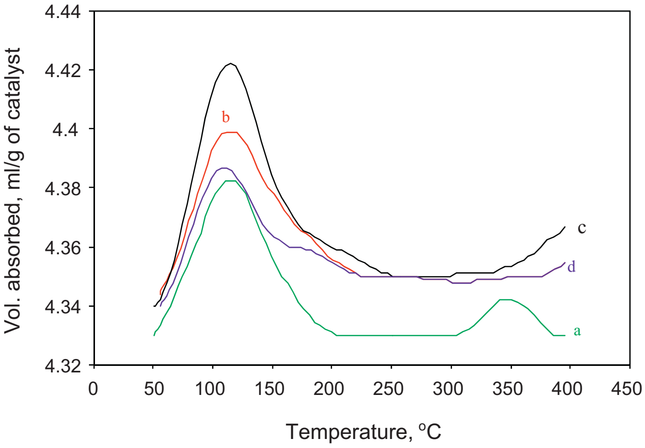

Fig. 3 – Carbon dioxide TPD profiles for various catalysts (a) K–OMS-2, (b) 5%Ag–OMS-2, (c) 10% Ag–OMS-2, (d) 15%Ag–OMS-2.

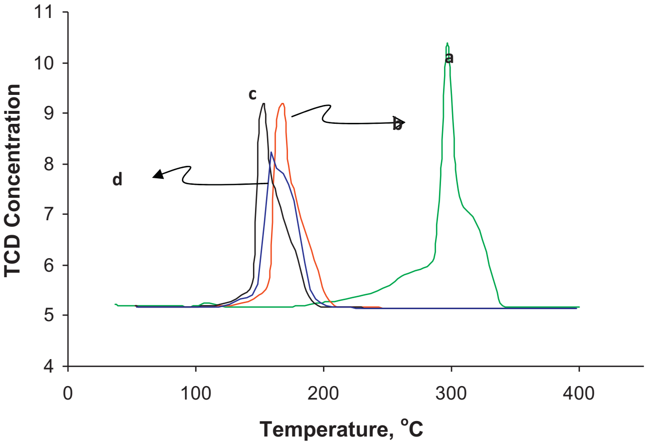

Fig. 4 – TPR profiles for various catalysts (a) K–OMS-2, (b) 5%Ag–OMS-2, (c) 10% Ag–OMS-2, (d) 15%Ag–OMS-2.

et al., 2003; Ramos et al., 2008). TPR studies also confirm the silver existence in the catalyst.

To ascertain the stability of the catalyst and effect of oxidation and reduction cycle, TPR was carried out twice with intermediate oxidation and degassing followed by TPR. There was no major change in TPR profile. It indicates that reduction and oxidation cycle does not alter the structure of the catalyst. Presence of silver increases the weak acidity (observed by TPD–NH$_3$ profile) and reduces reduction temperature (observed from TPR profile) which enhances the reduction-oxidation cycle and performance of the catalyst.

With addition of any extra metal/metal oxides leads to the surface area and pore volume reduction. However, in this work as reported in Table 1, surface area and pore volume increases with increase in silver loading from 5 to 15%. This is only feasible due to change in structure of the catalyst surface morphology and smaller size of Ag$^+$ than K$^+$. Similar phenomena was also observed by Jothiramalingam et al. (2005).

Fig. 5 depicts SEM of three catalyst samples, which confirm the presence of nano fibrous structure. Surface morphology of K–OMS-2 remains unaltered even after addition of silver. This confirms that silver was deposited inside the pores of the catalyst. The presence of silver inside the catalyst was further confirmed by the EDX analysis (Table 2).

The XRD patterns of K–OMS-2 and Ag–OMS-2 show a well crystalline cryptomelane structure which is a characteristic of octahedral molecular sieves (Fig. 6). The set of (1 0 1), (0 0 2), (3 0 1), (2 1 1), (3 1 0), (1 1 4) and (6 0 0) reflections at $2\theta = 12.23$, 17.93, 28.45, 37.24, 41.62, 49.59 and 59.90 are characteristic peaks of the K–OMS-2 structure (JCPDS card number 29-1020). JCPDS card number 77-1987 for silver hollandite (Ag$_{1.8}$Mn$_8$O$_{16}$) shows that it is characterized by strong reflections (2 2 0), (1 3 0), (1 0 1), (2 1 1), (2 4 0), (2 3 1) and (1 4 1) corresponding to 2θ values of 25.892, 29.012, 32.342, 37.375, 41.492, 46.0029 and 49.91, respectively. In our case, the intensity of two new peaks at 2θ values of 32.09 and 46.12 has increased with an increase in silver loadings, which further confirm existence of silver ions in the framework. The diffraction lines at 32.09 and 46.12 suggest the formation of Ag–hollandite by substitution of K by

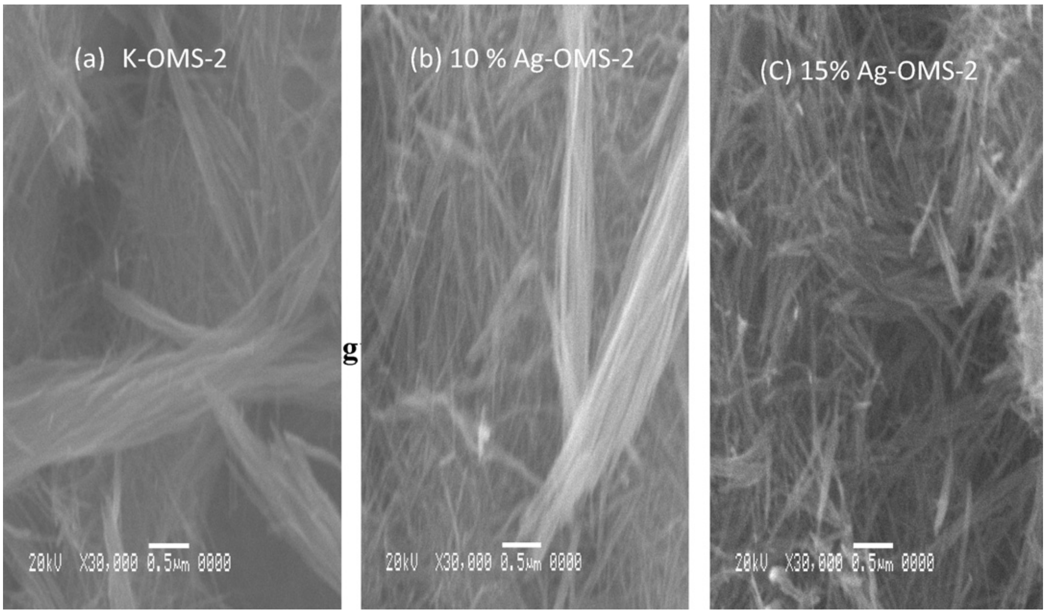

Fig. 5 – SEM Images of catalysts K–OMS-2, (b) 10% Ag–OMS-2, (c)15%Ag–OMS-2.

Table 1 – Surface area analysis of various catalysts.

Catalyst	BET surface area, m^2/g	Langmuir surface area, m^2	BJH adsorption pore volume, cm^3/g
K–OMS-2	89.1	150.4	0.463
5% Ag–OMS-2	100.1	165.2	0.518
10% Ag–OMS-2	110.7	185.3	0.589
15% Ag–OMS-2	118.6	199.9	0.659

Table 2 – EDX analysis.

Element	Mass %			
	K–OMS-2	5% Ag–OMS-2	10% Ag–OMS-2	15%Ag–OMS-2
O	29.1	33.4	33.6	34.4
K	4.2	3.8	2.6	1.5
Mn	66.0	58.4	55.0	50.8
Ag	0	4.3	8.3	12.9

Ag inside the 2 × 2 tunnels formed by the octahedral MnO_6. Thus, Ag is part of the structure but is not substituting Mn in the octahedral framework. Our findings are consistent with recent characterization of silver loaded OMS-2 by others (Chen et al., 2007; Gac, 2007; Gac et al., 2008).

3.2. Oxidation reaction

3.2.1. *Effect of diluant*

Oxidation of 1-octanol was carried out with toluene as a diluant and also without any solvent using 10% Ag–OMS-2 (Table 3). A blank experiment was also done with toluene alone in presence of catalyst under the same reaction conditions to test if any toluene could get oxidized. There was no conversion of toluene in presence of catalyst under given reaction conditions. An experiment without the catalyst was also carried out to observe that there was no conversion in the absence of catalyst.

When pure 1-octanol was used, there was over-oxidation of the product 1-octanal to octanoic acid.

$$\underset{\text{1-Octanol}}{CH_3(CH_2)_7OH} \xrightarrow{O_2} \underset{\text{1-Octanal}}{CH_3(CH_2)_6CHO} \xrightarrow{O_2} \underset{\text{1-Octanoic acid}}{CH_3(CH_2)_6COOH}$$

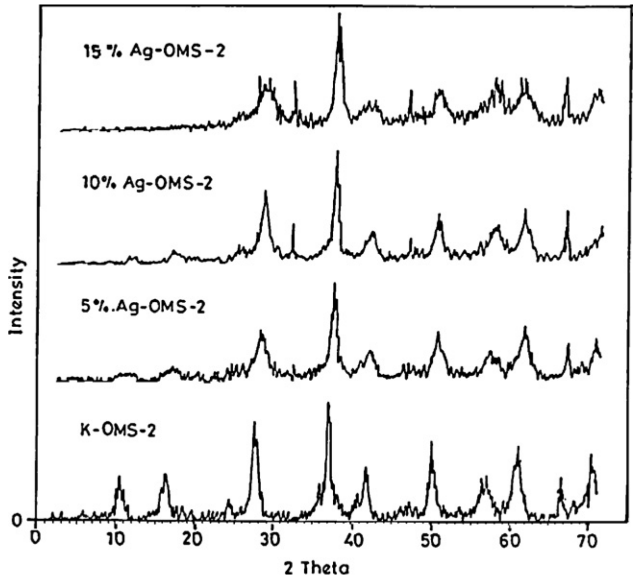

Fig. 6 – XRD Patterns of catalyst samples and effect of silver incorporation.

Dilution of 1-octanol with toluene was found to suppress the formation of 1-octanoic acid since it reduced the partial pressure and also improved the selectivity of the 1-octanal significantly. Toluene increases the desorption rate of the 1-octanal from the catalyst surface and reduces over- oxidation and catalyst deactivation. Hence further experiments were conducted with toluene as a diluant.

Use of nitrogen can be a good option for cost and from ease of separation point of view. Selectivity of the 1-octanal is a critical issue. With pure 1-octanol and high gas flow rate, the selectivity was substantially reduced. So partial pressure of 1-octanol in vapour phase is very critical. To achieve the same partial pressure equivalent to toluene–octanol system, volume or quantity of the nitrogen required (considering ideal vapor mixture which follows Roults law), large flow of inert gas creates problem in downstream separation of product from the inert gas. Selectivity of desired product was also reduced in case of nitrogen–octanol system. Whereas in case of toluene, being organic molecule it possesses similar affinity for adsorption and so it helps in desorption of desired product molecule from the surface of the catalyst. However, on a plant scale, toluene needs to be avoided.

3.2.2. *Catalyst screening*

Table 4 compares the efficacies of various catalysts in the oxidation of 1-octanol vis-à-vis the current work. Liquid phase oxidation gives better activity and selectivity at a lower concentration. However, at higher concentration, conversion and selectivity decreases significantly. Compared to silver metal catalyst, silver loaded OMS-2 gives better activity and selectivity at lower operating temperature. So Ag–OMS-2 was selected for further study. Fig. 7 shows the activity and selectivity of various catalysts used in air oxidation of 1-octanol in vapour phase. All these catalysts were synthesized in our laboratory. UDCaT-3 is also a redox material based on OMS-2 containing vanadium (Yadav and Maniar, 2008). 10% Ag–OMS-2 shows the highest selectivity with very high conversion of 1-octanol.

Addition of silver inside the framework of the catalyst surface improves the activity and selectivity of the catalyst significantly. These results confirm the synergistic effect of the silver in presence of Mn and K ions present in the catalyst. An increase in silver loading from 5% to 10% increases the activity of the catalyst significantly. However, increment from 10% to 15% does not show any significant improvement. On the contrary, selectivity to 1-octanal decreases significantly. But further increase in silver loading, 15% reduction in weak acid

Table 3 – Effect of diluent on conversion and selectivity.

Diluent	Flow rate of 1-octanol, mol h^{-1}	Air flow rate, L/h	1-Octanol Conversion %	Selectivity to 1-Octanal+ %
Solventless	0.06175	6	30.0	65.2
Toluene[a]	0.08393	6	75.5	95

Reaction conditions: 10% Ag–OMS-2: 0.5 g, temperature: 325 °C, pressure: 101.3 kPa,, 16.74 h^{-1} WHSV: 16.74 h^{-1}.

[a] Molar ration of toluene to 1-octanol: 4:1, +remaining 1-octanoic acid.

site takes place. Further, the number of sites available for the reaction would be more than required. Additional sites lead to overoxidation to 1-octanoic acid. High concentration of the silver inside the catalyst surface does not favour the 1-octanol oxidation reaction. Further study was carried out with 10% Ag–OMS-2 catalyst.

3.2.3. *Effect of external and internal mass transfer resistance*

Effect of external and internal mass transfer resistance were tested under reaction conditions. Catalyst weight and feed flow rate were maintained in such a way that no temperature gradient was observed across the catalyst bed. Effect of

Table 4 – Comparison of various catalyst used for 1-octanol oxidation.

No.	Catalyst	Reaction conditions	Conversion of 1-octanol, %	Selectivity to 1-octanal, %	Reference
1.	10%Ag–OMS-2	Catalyst- 0.5 g, 598 K, toluene to 1-octanol molar ratio- 4:1, WHSV-16.74 h^{-1}, air flow rate- 6 L/h, 101.3 kPa, $W/F_{A0} = 20$	75.6	96.0	This work
2.	$Ru_{0.45}Co_{0.36}/TiO_2$	Ru -1 mol%, 1-octanol-1 mmol, 353 K, O_2-404 kPa, $C_2H_4Cl_2$-30 mL, 3 h.	100	>99	Kockritz et al. (2006)
3.	Platinum group metal (PGM)	1-Octanol in toluene -15 mmol, reactant:metal molar ratio- 80:1, 5% Pt, 1%Bi/C, 333 K, air -304 kPa, 20 rps, 30 min	89	15	Anderson et al. (2003)
4.	Mono-ruthenium-substituted silicotungstate,	1-Octanol-1 mmol, Isobutyl acetate- 3 mL, 383 K, O_2, 48 h.	Yield 14, Turn over number 207	44 (n-Octanoic acid 30%).	Yamaguchi and Mizuno (2002)
5.	$MnFe_{1:5}Ru_{0:35}Cu_{0:15}O_4$	1-Octanol-2 mmol, catalyst- 0.3 g, Ru-0.42 mmol, toluene-5 mL, room temperature, air, 7 h.	51	51	Ji et al., 2002
6.	0.15 mmol of $Zr(O\text{-}t\text{-}Bu)_4$ or $Zr(O\text{-}n\text{-}Pr)_4$/*tert*-butyl hydroperoxide/3 Å molecular sieves	1-Octanol-1.5 mmol, 3 mmol anhydrous TBHP in CH_2Cl_2, 0.6 g activated molecular sieves, 333 K, 2 h.	98	80	Krohn et al. (1996)
7.	Metal silver catalyst	1-Octanol flow rate -0.0214 mol h^{-1}, 873 K, air- 20 mL/min, molar ratio of alcohol/O_2 -2	70	98	Yang et al. (2005)
8.	1% Pd/MgO catalyst	1-Octanol-1 mmol, catalyst-0.10 g, 0.0094 mmol Pd, TFT-1.5 mL, 343-353 K, O_2, 20 h	20	100	Pillai and Demessie, 2004
9.	Aluminum hydroxide-supported palladium (2 mol% Pd) catalyst	1-Octanol-1.00 mmol in 2 mL of TFT, 373 K, air-101 kPa, 12 h.		19	Kwon et al., 2005
10.	Cu/MgO	1-Octanol-2 mmol, styrene- 8 mmol, catalyst -200 mg, mesitylene- 8 mL, N_2 atmosphere, 423 K, 4 h.	65	>99	Shi et al., 2010
11.	Ru^{3+}-exchanged hydroxyapatite (RuHAP)	1-Octanol- 2 mmol, RuHAP-0.2 g, toluene-5 mL, 333 K, O_2, 16 h	95	94	Yamaguchi et al. (2000)

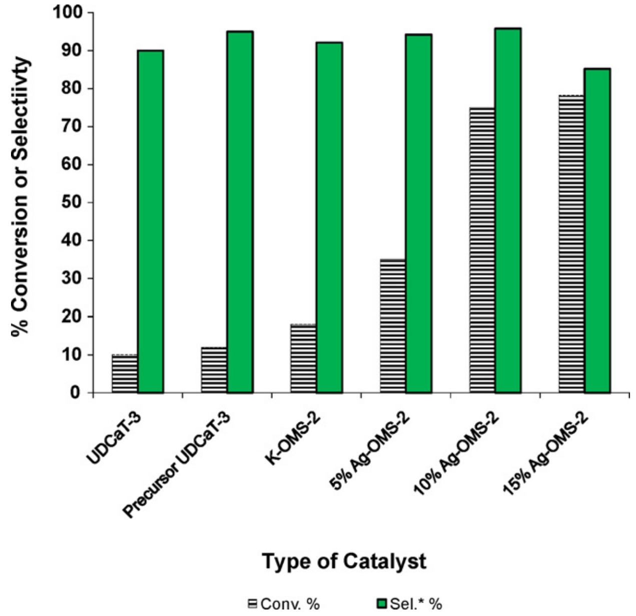

Fig. 7 – Catalyst screening for 1-octanol oxidation Reaction conditions: Catalyst loading- 0.5 g, temperature- 325 °C, toluene to 1-octanol molar ratio- 4:1, air flow rate: 6 L/h, WHSV-16.74 h^{-1}, pressure –101.3 kPa.

external and internal mass transfer resistance were tested under reaction conditions (Fig. 8). Effect of external mass transfer resistance was carried out by varying mass flow rate of the feed by keeping the W/F_{A0} ratio the same. There was no significant difference between two conversion levels of the different mass flow rates. Similarly the influence of internal diffusion resistance was evaluated by varying the catalyst particle size. Experiments were carried out with two different particle sizes of 0.01 and 1 mm. The conversion was practically the same with both the particle sizes. The Wiesz–Prater modulus, C_{WP}, was calculated based on the effective diffusivity and observed reaction rate. The value of C_{WP} was 0.05 for effective diffusivity value of 10^{-11} m^2/s, which is a conservative estimate. Since $C_{WP} \ll 1$, there was no intra-particle diffusion resistance. Thus, the reaction was intrinsically kinetically controlled. This is also bolstered by the high value of activation energy.

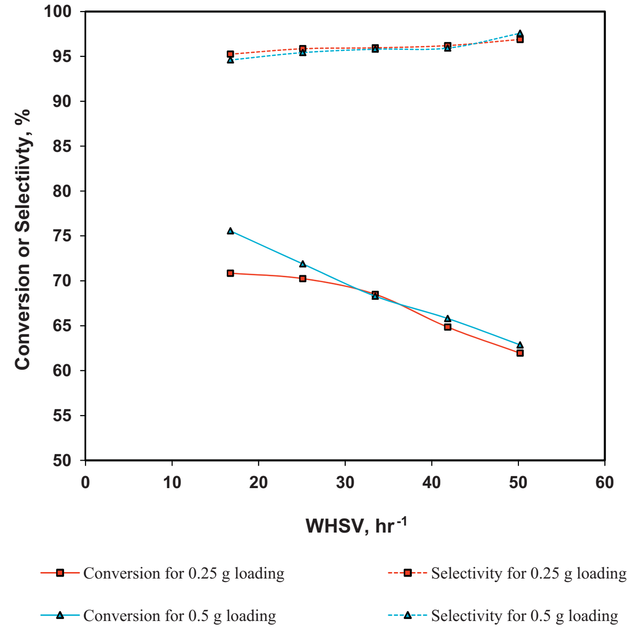

Fig. 8 – Effect of external mass transfer on conversion and selectivity Reaction conditions:10% Ag–OMS-2 Catalyst loading- 0.5 g, temperature- 325 °C, toluene to 1-octanol molar ratio- 4:1, air flow rate: 6 L/h, pressure –101.3 kPa. All results are at the end of 2 h.

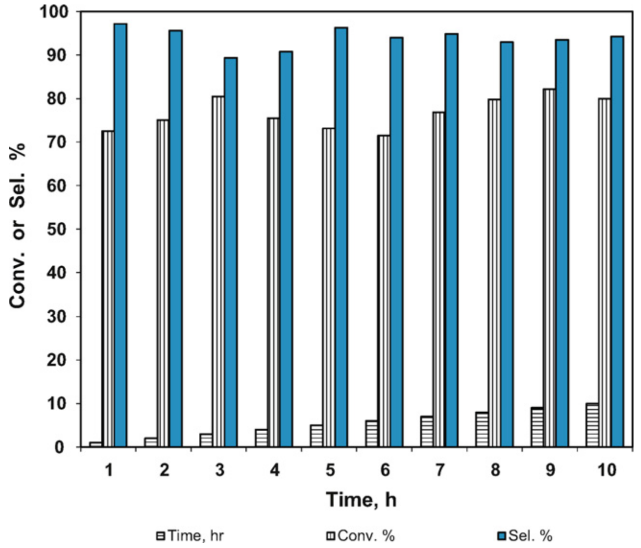

Fig. 9 – Time on stream studies to test activity and stability of catalyst Reaction conditions: 10% Ag–OMS-2 Catalyst loading- 0.5 g, temperature- 325 °C, toluene to 1-octanol molar ratio- 4:1, air flow rate: 6 L/h, WHSV-16.74 h^{-1}.

3.2.4. *Time on stream data (TOS)*

The activity and stability of the catalyst was verified by collecting the TOS data for 10 h (Fig. 9). The catalyst remained stable and active without any appreciable loss in activity and selectivity for the 1-octanal.

3.2.5. *Reuse and regeneration of catalyst*

After completion of the reaction under given conditions, in situ regeneration of the catalyst was carried out. During regeneration, temperature of the catalyst bed was increased up to 623 K and methanol vapour was passed along with air. It was activated under the flow of air at the reaction temperature for 2 h before reusing. Fig. 10 shows that there is no appreciable decrease in the activity and selectivity remain constant even after 4th reuse of the catalyst. Thus, 10%, w/w Ag–OMS-2 possesses very good regeneration and reusability characteristics.

3.2.6. *Effect of air flow rate*

Air flow rate was varied from 4 to 10 L/h (Fig. 11). At WHSV of 16.74 h^{-1}, the conversion increased up to 6 L/h and thereafter it decreased. It is due to the right air to 1-octanol molar ratio. An air flow rate beyond 6 L/h decreased the conversion due to decrease in residence time. At WHSV of 50.21 h^{-1}, the conversion increased continuously with increasing air flow rate, since the residence time increased correspondingly. In both cases, at low air flow rate, the selectivity was very high, beyond 96 and 98% for WHSV of 16.74 and 50.21 h^{-1}, respectively and decreased slightly as the flow rate was increased.

3.2.7. *Effect of toluene to 1-octanol molar ratio*

Toluene to 1-octanol molar ratio was varied from 2:1 to 6:1 (Fig. 12). Selectivity to 1-octanal increased with increase in

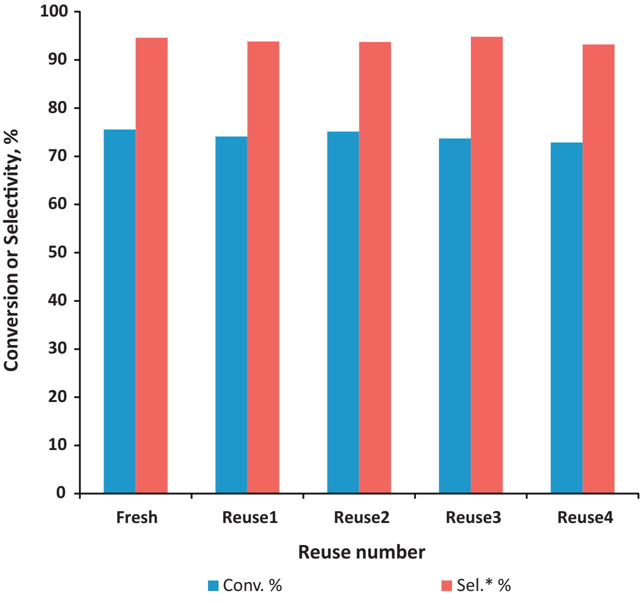

Fig. 10 – Effect of catalyst reusability on conversion and selectivity reaction conditions: 10% Ag–OMS-2 Catalyst loading- 0.5 g, temperature- 325 °C, toluene to 1-octanol molar ratio- 4:1, air flow rate: 6 L/h, WHSV-16.74 h^{-1}, pressure −101.3 kPa. All results are at the end of 4 h.

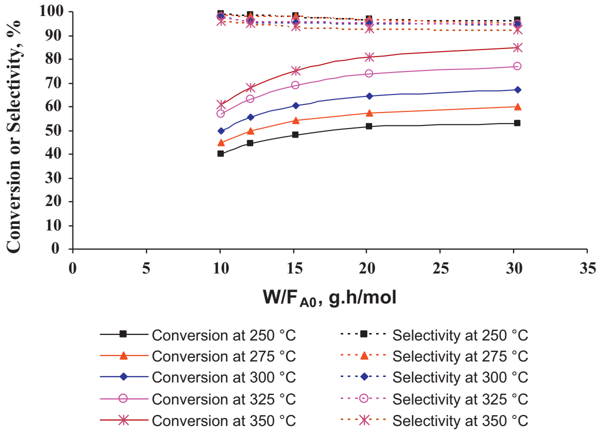

Fig. 12 – Effect of toluene to 1-octanol molar ratio on conversion and selectivity Reaction conditions: 10% Ag–OMS-2 Catalyst loading- 0.5 g, temperature- 325 °C, toluene to 1-octanol molar ratio- 4:1, air flow rate: 6 L/h, all results are at the end of 2 h.

molar ratio from 2:1 to 6:1. Increasing WHSV at the same mole ratio of toluene to 1-octanol decreased the conversion and the selectivity increased. This is due to suppression of the overoxidation due to reduction in residence time. Greater than 95% selectivity was found at 4:1 molar ratio. With an increase in molar ratio beyond 4:1, there was no significant improvement in selectivity for 1-octanal.

Use of lower toluene to 1-octanol molar ratio results into higher partial pressure of 1-octanal which leads to oxidation of 1-octanal to octanoic acid. It also leads to catalyst deactivation. Higher concentration of toluene reduces the partial pressure of the 1-octanol and 1-octanal. Toluene also helps in desorption of the 1-octanal and other byproducts from the active sites of the catalyst surface. Thus presence of toluene increases the turn over number (TON) as well as catalyst life. Increase in molar ratio to 6:1 improves the selectivity slightly but economically it is not attractive. Increasing the toluene to 1-octanol molar ratio means increasing energy for distillation for solvent separation and increasing recycling cost of the solvent. Therefore the toluene to 1-octanol molar ratio was selected as 4:1 for further study.

3.3. *Effect of temperature*

The effect of W/F$_{A0}$ on conversion and selectivity was studied at different temperatures varying from 523 to 623 K (Fig. 13) was done with 10% Ag–OMS-2. With increase in temperature, the conversion increases but selectivity decreases slightly. Even at a higher temperature of 623 K, the selectivity to 1-octanal was >95%. The increase in conversion with temperature at a given W/F$_{A0}$ also demonstrates that the reaction is intrinsically kinetically controlled.

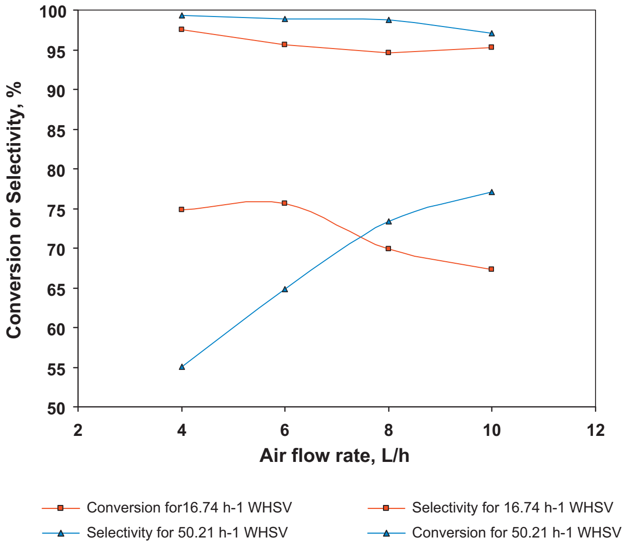

Fig. 11 – Effect of Air flow rate on conversion and selectivity Reaction conditions: 10% Ag–OMS-2 Catalyst loading- 0.5 g, temperature- 325 °C, toluene to 1-octanol molar ratio- 4:1, air flow rate: 6 L/h, WHSV-16.74 h^{-1}, pressure −101.3 kPa. All results are at the end of 2 h.

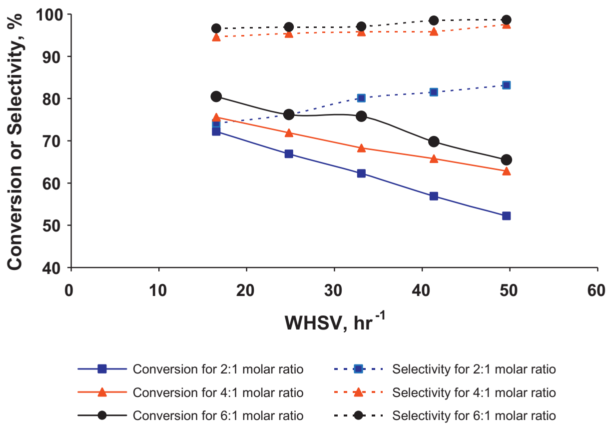

Fig. 13 – Effect of temperature on conversion and selectivity reaction conditions: 10% Ag–OMS-2 Catalyst loading- 0.5 g, temperature- 325 °C, toluene to 1-octanol molar ratio- 4:1, air flow rate: 6 L/h, all results are at the end of 2 h.

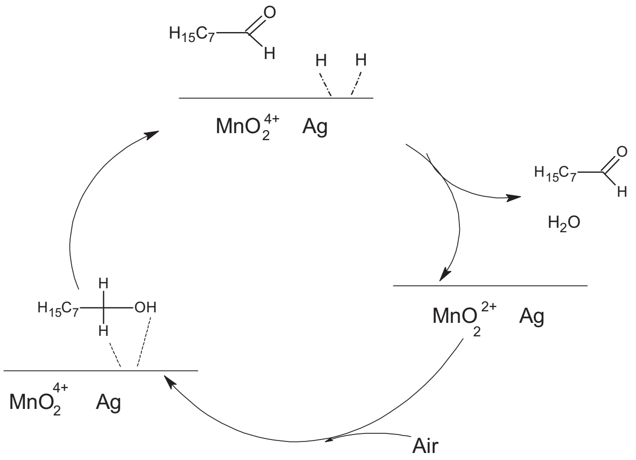

Fig. 14 – Mars–van Krevelen mechanism for 1-octanol oxidation.

3.4. Reaction mechanism

Participation of lattice oxygen from the surface of K–OMS-2 during the oxidation reaction was suggested and proved by Makwana et al. (2002). Mars–van Krevelen mechanism involves the participation of surface oxygen in the reaction and subsequently surface is regenerated with the oxygen supply source like air or oxygen, etc. (Fig. 14). Based on this mechanism, a suitable model is derived for the vapour phase air oxidation of 1-octanol.

Reaction of substrate with lattice oxygen:

$$C_8H_{17}OH+\boxed{O}\rightarrow C_7H_{16}CHO+\ H_2O+\square \tag{4}$$

The vacant lattice site is shown as $\square$

Regeneration of the empty space of lattice with oxidant like air:

$$2\square+O_2\rightarrow 2\,\boxed{O} \tag{5}$$

3.5. Kinetic model

Using above mechanism a suitable kinetic model was derived.

Rate of oxidation of the 1-octanol, $-r_A$, (mol gcat^{-1} h^{-1}) is derived as follows:

$$-r_A=\frac{dx_A}{d(W/F_{A_0})}=k_1P_{A_0}(1-x_A)\theta \tag{6}$$

where, θ = degree of catalyst surface occupied by the oxygen k_1 = rate constant for the 1-octanol oxidation reaction, mol gcat^{-1} h^{-1} m^2 N^{-1} P_{A_0} = partial pressure of 1-octanol at starting of the reaction, N/m2 x_A = fractional conversion of 1-octanol at given W/F_{A0} value (–), W = weight of the catalyst, g, F_{A_0} = molar flow rate of reactant, 1-octanol, mol/h

Rate of re-oxidation of the catalyst is given by the following Eq. (4):

$$-r_{O_2}=k_2P_{O_2}(1-\theta) \tag{7}$$

where, k_2 = rate constant for the reaction for re-oxidation of the catalyst, mol gcat^{-1} h^{-1} m^2 N^{-1} P_{A_0} = partial pressure of oxygen, N/m^2 $1-\theta$ = degree of catalyst surface unoccupied by the oxygen.

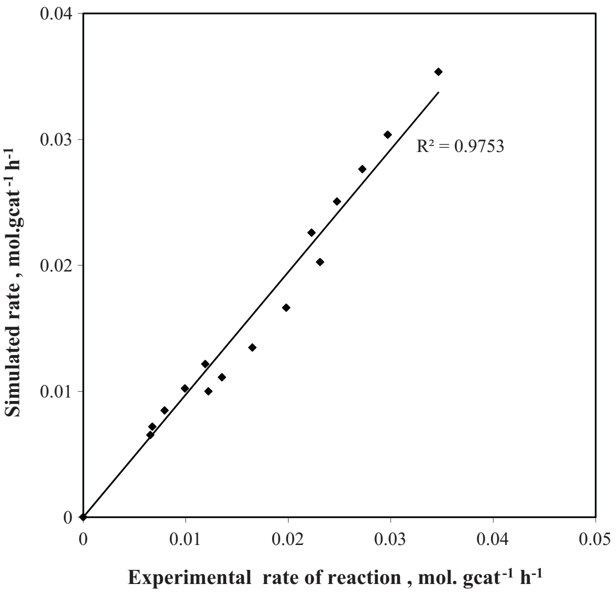

Fig. 15 – Parity plot for experimental vs. simulated rates.

$$\text{At steady state conditions,}\ \frac{-r_A}{2}=-r_{O_2} \tag{8}$$

From Eqs. (6)–(8),

$$\frac{k_1P_{A_0}(1-x_A)\theta}{2}=k_2P_{O_2}(1-\theta) \tag{9}$$

Simplifying Eq. (9) in terms of θ, and substituting the values of θ in Eq. (6), the following is obtained:

$$-r_A=\frac{dx_A}{d(W/F_{A_0})}=\frac{1}{1/\left[k_1P_{A_0}(1-x_A)\right]+0.5/\left[k_2P_{O_2}\right]} \tag{10}$$

If change in partial pressure of oxygen is considered as small and rate of regeneration of lattice surface through available oxygen from gas phase is very fast, second term in the denominator remains constant and Eq. (10) reduces to:

$$-r_A=\frac{dx_A}{d(W/F_{A_0})}=\frac{1}{1/\left[k_1P_{A_0}(1-x_A)\right]+0.5/C} \tag{11}$$

where $C=k_2P_{O_2}$ = Constant and hence,

$$-r_A=\frac{dx_A}{d(W/F_{A_0})}=\frac{k_1P_{A_0}(1-x_A)}{1+(0.5/C)k_1P_{A_0}(1-x_A)} \tag{12}$$

Eq. (12) is further simplified to:

$$-r_A=\frac{dx_A}{d(W/F_{A_0})}=\frac{k_1P_{A_0}(1-x_A)}{1+C'k_1P_{A_0}(1-x_A)} \tag{13}$$

where, k_1 = apparent rate constant, mol gcat^{-1} h^{-1}m^2 N^{-1}

$$C'=\frac{0.5}{C}=\text{Constant.}$$

A nonlinear regression analysis was carried out by using Langrange–Marquade method (Polymath 5.1). The values of rate constants were extracted as at different temperatures. A parity plot of experimental vs. simulated rates at different temperature is given in Fig. 15. There is an excellent

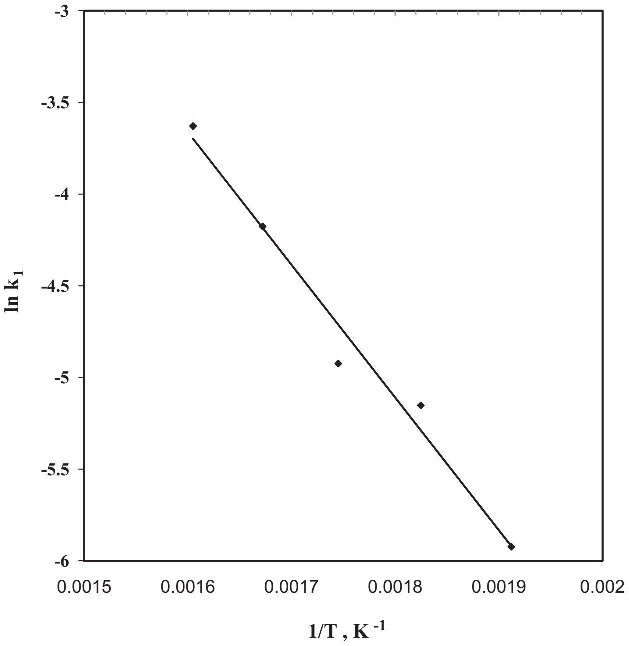

Fig. 16 – Arrhenius plot for 1-octanol oxidation.

fit between the observed and calculated values of rate data, thereby proving the validity of the Mars–van Krevelen mechanism. The Arrhenius plot was made to get the activation energy for the 1-octanol oxidation as 14.39 kcal/mol (Fig. 16). This value also suggests that the vapour phase oxidation of 1-octanol using 10% Ag–OMS-2 catalyst is intrinsically kinetically controlled.

4. Conclusions

Vapour phase oxidation of 1-octanol to 1-octanal is commercially attractive and the use of a novel catalyst was investigated in this work. Cryptomelane type octahedral molecular sieve type 2 (K–OMS-2) was modified by substituting K with Ag inside its framework using different loadings of Ag. The catalyst activity showed significant improvement with increases in Ag loading from 5 to 15%, w/w. All catalysts were characterized to understand the activity and selectivity. 1-Octanol oxidation with air at atmospheric pressure with 10% Ag–OMS-2 shows the highest selectivity for 1-octanal. Toluene to 1-octanol molar ratio plays a key role in improving selectivity for 1-octanal. The catalyst is stable and can be regenerated without difficulty and its fidelity is maintained during regeneration. Reaction conditions were optimized and kinetic study was carried out. The optimized conditions are: $W/F_{A0} = 20$ g h/mol, 523 K, toluene to 1-octanol molar ratio- 4:1, WHSV-16.74 h^{-1}, air flow rate- 6 L/h, air pressure- 101.3 kPa. The reaction follows the Mars–van Krevelen mechanism. The activation energy for air oxidation of 1-octanol found was 14.39 kcal/mol using 10% Ag–OMS-2. This work provides a better catalytic process than reported so far and it is a green process.

Acknowledgements

G.D. Yadav acknowledges support from the Darbari Seth Professor and R.T. Mody Professor Endowments, and Department of Science and Technology (Govt of India) as J.C. Bose National Fellow. R.K. Mewada received a Senior Research Fellowship (SRF) from University Grant Commission, New Delhi.

References

Anderson, R., Griffin, K., Johnston, P., Alsters, P.L., 2003. Selective oxidation of alcohols to carbonyl compounds and carboxylic acids with platinum group metal catalysts. Adv. Synth. Catal. 345, 517–523.

Bogda, D., Lukasiewicz, M., 2000. Microwave-assisted oxidation of alcohols using aqueous hydrogen peroxide. Synletter 1, 143–145.

Buffin, B.P., Clarkson, J.P., Belitz, N.L., Kundu, A., 2005. Pd(II)-biquinoline catalyzed aerobic oxidation of alcohols in water. J. Mol. Catal. A: Chem. 225, 111–116.

Che, C.M., Yip, W.P., Yu, W.Y., Ruthenium, 2006. Catalyzed oxidation of alkenes, alkynes, and alcohols to organic acids with aqueous hydrogen peroxide. Chem. Asian J. 1, 453–458.

Chen, J., Tang, X., Liu, J., Zhan, E., Li, J., Huang, X., Shen, W., 2007. Synthesis and characterization of Ag–hollandite nanofibers and its catalytic application in ethanol oxidation. Chem. Mater. 19 (17), 4292–4299.

Coleman, K.S., Coppe, M., Thomas, C., Osborn, J.A., 1999. Catalytic oxidation of alcohols into aldehydes and ketones by an osmium-copper bifunctional system using molecular oxygen. Tetrahedron Lett. 40, 3723–3726.

Ciriminna, R., Pagliaro, M., 2010. Industrial oxidations with organocatalyst TEMPO and its derivatives:. Org. Process Res. Dev. 14 (1), 245–251.

Einhorn, J., Einhorn, C., Ratajczak, F., Pierre, J.L., 1996. Efficient and highly selective oxidation of primary alcohols to aldehydes by n-chlorosuccinimide mediated by oxoammonium salts. J. Org. Chem. 61, 7452–7454.

Franz, G., Sheldon, R.A., 2003. Ullamann's Encyclopedia of Industrial Chemistry, 24, p. 489.

Fritz-Langhals, E., 2005. Technical production of aldehydes by continuous bleach oxidation of alcohols catalyzed by 4-hydroxy-TEMPO. Org. Process Res. Dev. 9, 577–582.

Fu, Q., Kudriavtseva, S., Saltsburg, H., Stephanopoulos, M.F., 2003. Gold–ceria catalysts for low-temperature water–gas shift reaction. Chem. Eng. J. 93, 41–53.

Gac, W., 2007. The influence of silver on the structural, redox and catalytic properties of the cryptomelane-type manganese oxides in the low-temperature CO oxidation reaction. Appl. Catal. B: Environ. 75 (1–2), 107–117.

Gac, W., Giecko, G., Pasieczna-Patkowska, S., Borowiecki, T., Kepinski, L., 2008. The influence of silver on the properties of cryptomelane type manganese oxides in N_2O decomposition reaction. Catal. Today 137 (2–4), 397–402.

Gamez, P., Arends, I.W.C.E., Reedijka, J., Sheldon, R.A., 2003. Copper(II)-catalysed aerobic oxidation of primary alcohols to aldehydes. Chem. Commun., 2414–2415.

Gilhespy, M., Lok, M., Baucherel, X., 2005. Polymer-supported nitroxyl radical catalyst for selective aerobic oxidation of primary alcohols to aldehydes. Chem. Commun., 1085–1086.

Graaf, D., Franciscus, T. Euro. Pat. 0037149 A1, 1981.

Ji, H.B., Ebitani, K., Mizugaki, T., Kaneda, K., 2002. Environmentally friendly alcohol oxidation using heterogeneous catalyst in the presence of air at room temperature. Catal. Commun. 3, 511–517.

Jothiramalingam, R., Viswanathan, B., Varadarajan, T.K., 2005. Preparation, characterization and catalytic properties of cerium incorporated porous manganese oxide OMS-2 catalysts. Catal. Commun. 6, 41–45.

Kockritz, A., Sebek, M., Dittmar, A., Radnik, J., Bruckner, A., Bentrup, U., Pohl, M.M., Hugl, H., Magerlein, W., 2006. Ru-catalyzed oxidation of primary alcohols. J. Mol. Catal. A: Chem. 246, 85–99.

Krohn, K., Vinke, I., Adam, H., 1996. Transition-metal catalyzed oxidations 7. Zirconium-catalyzed oxidation of primary and secondary alcohols with hydroperoxides. J. Org. Chem. 61, 1467–1472.

Kwon, M.S., Kim, N., Park, C.M., Lee, J.S., Kang, Y.K., Park, J., 2005. Palladium nanoparticles entrapped in aluminum hydroxide: dual catalyst for alkene hydrogenation and aerobic alcohol oxidation. Org. Lett. 7, 1077–1079.

Makwana, V.D., Son, Y.C., Howell, A.R., Suib, S.L., 2002. The role of lattice oxygen in selective benzyl alcohol oxidation using oms-2 catalyst: a kinetic and isotope-labeling study. J. Catal. 210, 46–52.

Mallat, T., Baiker, A., 2004. Oxidation of alcohols with molecular oxygen on solid catalysts. Chem. Rev. 104, 3037–3058.

Matsumoto, T., Ueno, M., Wang, N.W., Kobayashi, S., 2008. Recent advances in immobilized metal catalysts for environmentally benign oxidation of alcohols. Chem. Asian J. 3, 196.

Miura, H., Watanabe, H., Ina, T., Nakjima, H. U.S. Pat. 6,642,419, B1, 2003.

Muzart, J., 2003. Palladium-catalysed oxidation of primary and secondary alcohols. Tetrahedron 59, 5789–5816.

Noyori, R., Aoki, M., Sato, K., 2003. Green oxidation with aqueous hydrogen peroxide. Chem. Commun., 1977–1986.

Pillai, U.R., Demessie, E.S., 2004. Selective oxidation of alcohols by molecular oxygen over a Pd/MgO catalyst in the absence of any additives. Green Chem. 6, 161–165.

Ramos, M.J., Jimenez, V., Funez, A., Romero, A., Sanchez, P., Valverde, J.L., 2008. Influence of the addition of a second metal on the catalytic performance of pt-beta agglomerated catalyst in the hydroisomerization of n -octane. Catal. Lett. 125, 220–228.

Sheldon, R.A., Kochi, J.K., 1981. Metal-Catalyzed Oxidations of Organic Compounds. Academic Press, New York.

Shi, R., Wang, F., Mu, X., Ta, N., Li, Y., Huang, X., Shen, W., 2010. Transfer dehydrogenation of 1-octanol to 1-octanal over Cu/MgO catalyst: effect of Cu particle size, Chinese. J. Catal. 31, 626–630.

Tanielyan, S.K., Augustine, R.L., Prakash, I., Furlong, K.E., Scherm, R.C., Jackson, H.E. WO 067484, 2004. (cf. CAN 141: 190314).

Tanielyan, S., Augustine, R., Meyer, O., Koreil, M. U.S. Pat. 7,030,279, 2006. (cf. CAN 144: 393182).

Yadav, G.D., Maniar, H.G., 2008. Synthesis of a novel redox material UDCaT-3: an efficient and versatile catalyst for selective oxidation, hydroxylation and hydrogenation reactions. Adv. Synth. Catal. 350, 2286–2294.

Yamaguchi, K., Mizuno, N., 2002. Heterogeneously catalyzed liquid-phase oxidation of alkanes and alcohols with molecular oxygen. New J. Chem. 26, 972–974.

Yamaguchi, K., Mori, K., Mizugaki, T., Ebitani, K., Kaneda, K., 2000. Creation of a monomeric ru species on the surface of hydroxyapatite as an efficient heterogeneous catalyst for aerobic alcohol oxidation. J. Am. Chem. Soc. 122, 7144–7145.

Yang, Z., Li, J., Yang, X., Xie, X., Wu, Y., 2005. Gas-phase oxidation of alcohols over silver: the extension of catalytic cycles of oxidation of alcohols in liquid-phase. J. Mol. Catal. A: Chem. 241, 15–22.

Zhan, B.Z., Thompson, A., 2004. Recent developments in the aerobic oxidation of alcohols. Tetrahedron 60, 2917–2935.

Zhou, H., Wang, J.Y., Chen, X., O'Young, C.L., Suib, S.L., 1998. Studies of oxidative dehydrogenation of ethanol over manganese oxide octahedral molecular sieve catalysts. Micropor. Mesopor. Mater. 21, 315–324.